DØ CALORIMETER UPGRADE

GREGORIO BERNARDI
LPNHE, Universités Paris VI/VII-IN2P3, 4,place Jussieu, 75252 Paris Cedex 05, France,
E-mail: gregorio@in2p3.fr

The upgrade of the DØ calorimeter system became necessary with the changes in the beam structure of the Tevatron and the introduction of a new tracking system, including a solenoid, in the DØ detector. In order to maintain the excellent performances of the DØ liquid Argon calorimeter, an exchange of its electronics, and the introduction of preshower detectors are currently undergoing.

1 Introduction

After the very successful Run I of the Tevatron, with about 100pb^{-1} accumulated from 1992 to 1996, which lead to the discovery of the Top quark in 1995, the improved performances of the machine and the detectors for the Run II will allow to focus on the physics potential at high p_T. Besides the increased discovery potential for the Higgs Boson or phenomena beyond the Standard Model, such as Supersymmetry or Contact Interactions, an integrated Luminosity of $\sim$ 2fb^{-1}/year opens the field for extended Top Quark studies and high precision measurements of electroweak parameters such as the W-mass. The improvement brought to the DØ detector [1] (see figure 1) with the Silicon Vertex Detector (SVX), the Central Fiber Tracker (CFT) and the presence of a magnetic field of 2T gives the necessary instrumentation for studying B physics and measure related parameters such as $\sin^2\beta$ with a precision of ~ 0.16. Finally further tests of QCD will complete the results from DIS-experiments in the understanding of the strong interaction.

With the construction of the new Main Injector and Recycler, the Tevatron delivers higher beam energies, 1TeV compared to 0.9TeV in Run I, and an increased luminosity from 10^{31}cm^{-2}s^{-1} in Run I to 10^{32}cm^{-2}s^{-1} in Run II. This is possible only by changing the beam structure and reducing the interaction time. Whereas during the Run I 6×6 bunches were spaced by $3.56\mu s$, allowing to form trigger signals and baseline samples in between interactions, the minimal gap size of 132ns in Run II, needs the use of fast electronics, signal pipelines, sophisticated trigger system and radiation hard detector components. Th variable bunch structure of 36 super-bunches being made of either 12 or 36 sub-bunches requires an additional flexibility of the Front-End and Read-Out electronics.

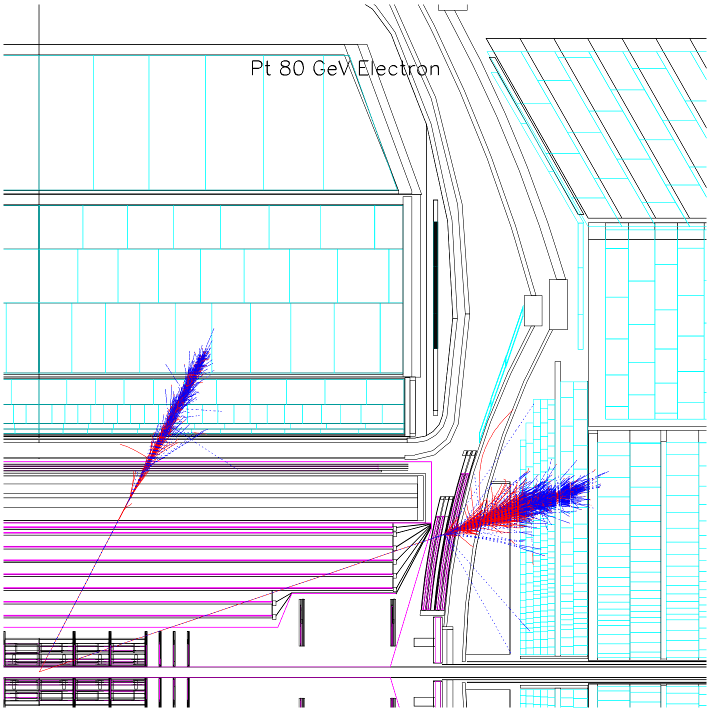

Figure 1. Simulation of electrons with $p_T = 80\mathrm{GeV}$ in central and forward region of the DØ Run II-detector. From inside out: the Silicon Vertex Detector (SVX), the Central Fiber Tracker (CFT) surrounded by the solenoid, the Central and Forward Preshowers (CPS and FPS) and the Central and Endcap Calorimeters (CC and EC).

2 The Preshower Detectors

The Central and Forward Preshowers serve to enhance the electron and photon identification and to sample energy after the solenoid coil, and thus serve as an additional calorimetric measurement. Figure 2 shows a sideview of the two subdetectors. The Central Preshower (CPS) [2] reaches out up to $\eta = 1.3$ and is made a of a lead layer tapered to the solenoid and three stereo layers of scintillator strips (u, v and z). The Forward Preshower (FPS) [3] on one Endcap Cryostat consists of two domes, assembled from azimuthal wedges, mounted on the cryostat of the Endcap Calorimeters and cover an η range between 1.5 and 2.5. For $\eta > 1.65$, which corresponds to the region where

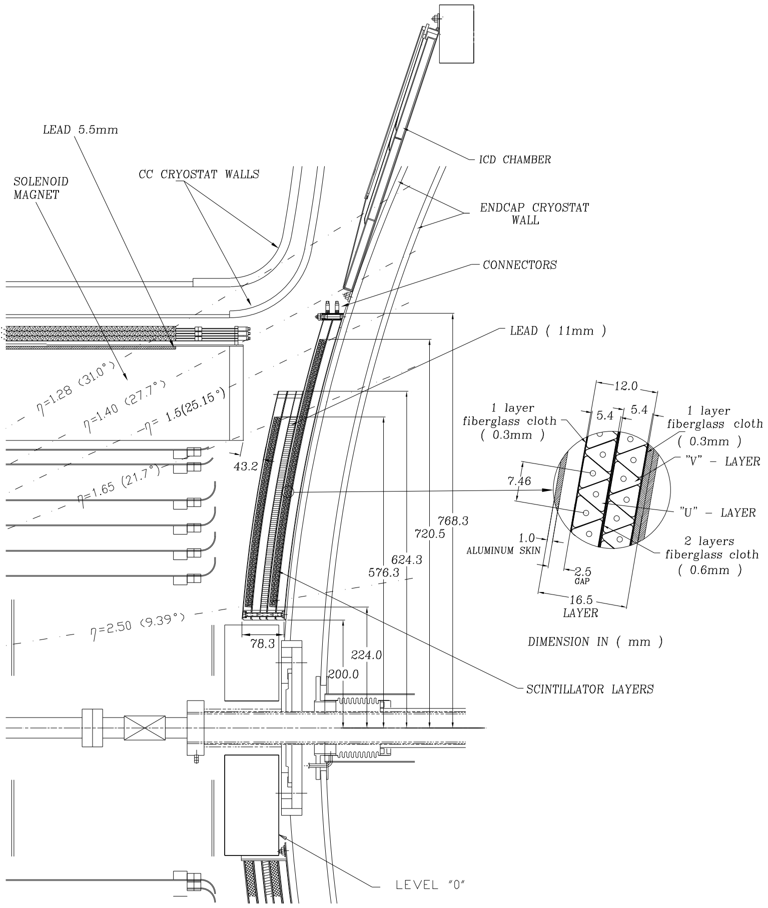

Figure 2. rz-view of the Central and Forward Preshowers (CPS and FPS).

particles do not encounter the solenoid, a $2X_0$ lead absorber is sandwiched in between the two domes, each dome containing two stereo layer of scintillator strips (u and v). The Read-Out of the Preshowers is done via Wavelength-Shifting Fibers (WLS), embedded among the scintillator strips, by Visible Light Photon Counters (VLPCs). The calibration of the Preshowers is ensured by a LED system.

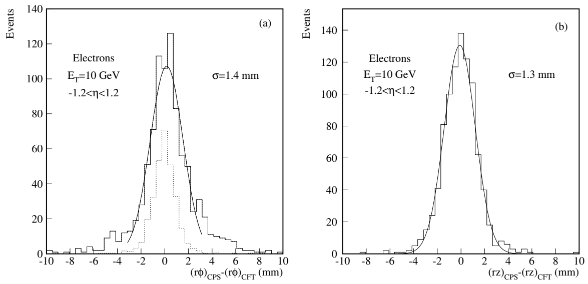

Figure 3. Position resolution in the $r\phi$ and rz lane of electrons with $E_T = 10$GeV comparing the measurement of the Central Preshower with the Central Fiber Tracker.

Figure 3 shows position reconstruction for electrons of $E_T = 10GeV$ Figure 2 shows position reconstruction for electrons of $E_T = 10GeV$ in the $r\varphi$ and rz planes, comparing the position measurements of the CFT with the one in the CPS. A resolution of $\sigma = 1.4$ in $r\varphi$ and and 1.3mm in rz is obtained..

The increased amount of dead material from the solenoid degrades the energy measurement in the CC, therefore the improvement using the CPS measurement is particularly important. Figure 4 shows the improvement of the energy reconstruction for soft electrons with $E_T = 2$GeV, comparing the reconstruction with and without the central preshower detector. For electrons of $E_T = 30$GeV $\sigma/E = 2.6\%$ is achieved.

Figure 5 is showing the shower profiles of 50 and 70GeV electrons as obtained from test beam data taken with a FPS prototype in 1997 at FNAL.

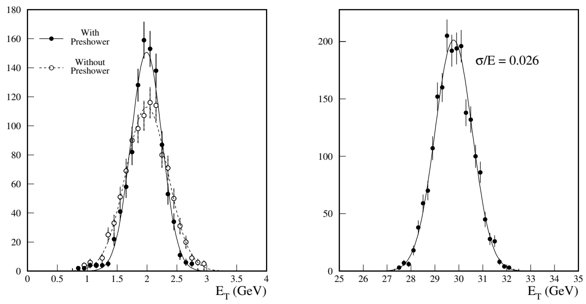

Figure 4. Simulation of the improvement obtained on the electron energy resolution with the DØ calorimeter including the Central Preshower detector for soft electrons at $E_T = 2$GeV and the energy measurement at $E_T = 30$GeV.

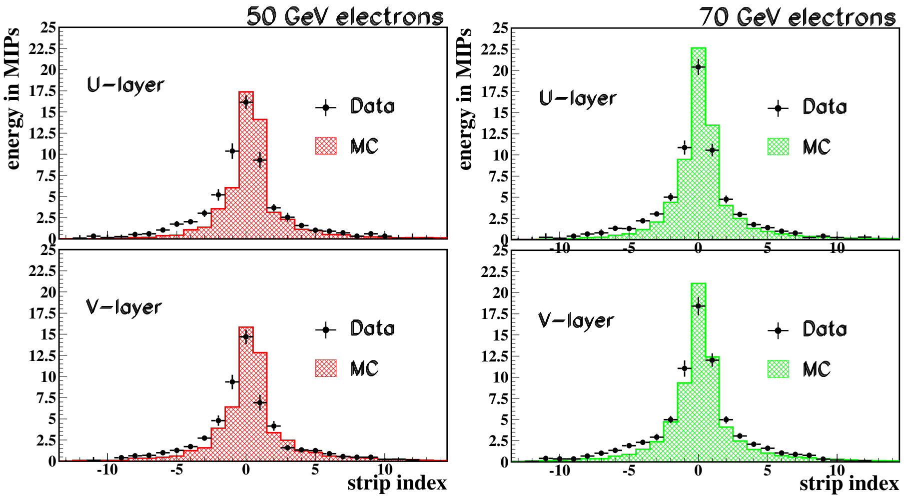

Figure 5. Shower Profiles of Electrons at $E = 50, 70$GeV for the U- and V-module layers in the FPS, comparing test beam measurements to the simulation.

Each plot is normalized to the corresponding MIP signal measured in the corresponding layer. The normalization is done independently for the data and the simulation, which is giving a good description of the measurement.

3 The Intercryostat Detector

Energy losses in between the cryostats of the CC and EC are diminished by measurement from the Intercryostat Detector (ICD), which improves therefore the jet energy and missing energy measurements. The ICD consists of 16 supertiles per CC/EC-region with a total of 384 scintillator tiles, covering a region of $1.1 < \eta < 1.4$. The scitillators are read out by Photo Multiplier Tubes (PMT) via WLS fibers. For the Run II, besides an increased acceptance, the ICD performance in the presence of a magnetic field and of the additional material from the solenoid had to be maintained. In order to reuse the existing PMT's, the light signal is brought via clear fibers to a region with low magnetic field.

4 The Calorimeter Electronics

A new design of the calorimeter electronics [4] became necessary in order to accommodate the bunch spacing from 3.5μs in Run I to 396 and even $132ns$ in Run II and to maintain level of noise and pile-up performance as in Run I. This implied the necessity to store the analog signal for 4μs, allowing to form the L1 trigger decision and to generate a separate, fast trigger signal for the calorimeter to be included in the L1 trigger level, and to adopt a new strategies for the Baseline Subtraction.

Figure 6 is sketching the calorimeter readout chain and the changes compared to the Run I setup. To minimize the sensitivity to reflections new impedance matched 30Ω signal cables replace the former 110Ω cables, between the detector and low noise preamplifiers. A fast trigger signal is then produced, whereas for the energy measurement a shaping of 400ns is applied. Switch Capacitor Arrays (SCA) store the signal until the L1 trigger decision is taken for up to $> 4\mu$s. The Baseline Subtracter (BLS) evaluates the 0-level three bunch crossings before the actual signal. New and additional controller were needed to coordinate the 144 analog samples per channel. Finally additional buffering for L2 and L3 trigger decisions is provided by supplementary SCA's. The increased power requirements are accommodated by using low noise commercial supplies. Finally a new calibration system to accommodate the timing constraints and improve the precision has been designed.

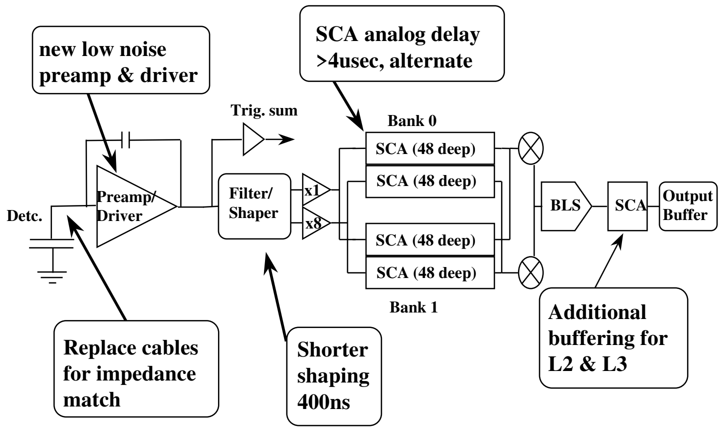

Figure 6. Read-out chain of the calorimeter in Run II indicating the replaced or additional components compared to the Run I electronics.

Figure 7 shows the new preamplifier, which is a hybrid circuit on ceramics, with 48 daughter cards on a single motherboard. The preamps are similar

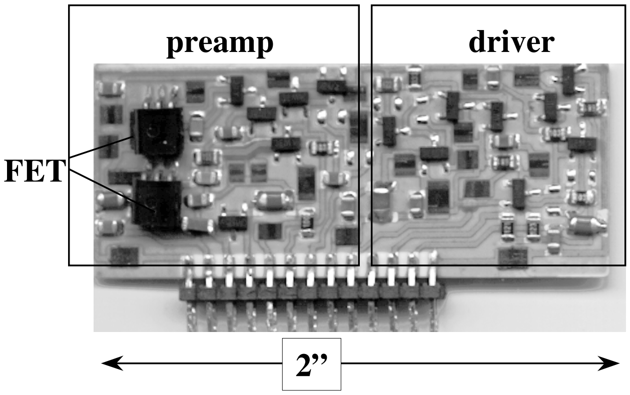

Figure 7. New calorimeter preamplifier daughter cards: indicated are the preamplifier with the 2 FET's and the driver.

to the previous one, except for the dual FET frontend, which improve the high frequency performance, due to a faster recovery time and compensate for detector capacitance. The new output drivers allow for terminated signal transmission.

A simplified schema of the SCA is shown in figure 8. The SCA is not designed for simultaneous read/write operations: two SCA banks alternate the reading and writing. It is approximately deadtimeless up to a L1 rate of

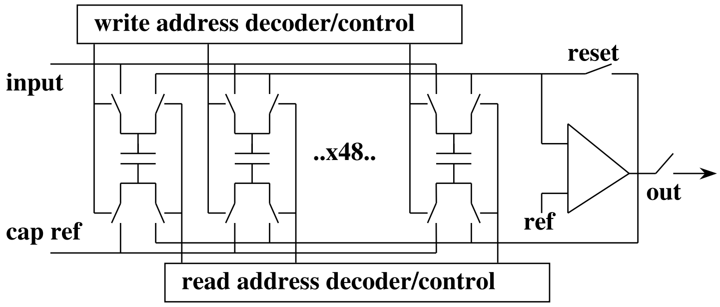

Figure 8. Layot of the Switch Capacitor Array (SCA) which provide storage of the analog signal for up to 4μs.

100kHz. The circuit has only a 12 bit dynamic range, but a low and high gain path for each readout channel ($\times 8/\times 1$) maintain the 15 bit dynamic range.

One of the main concerns designing the calorimeter electronics for Run II was to optimize the noise contributions in the new environment. The contribution from the electronics noise is increased due to the shorter shaping times as $\sqrt{t}$), from $2\mu s$ in Run I to $400ns$ in Run II, but decreases with the use of lower noise preamplifiers, the two FET input accounts for $1/\sqrt{2}$. The contribution from Uranium noise decreases due to the shorter shaping times as $\sqrt{t}$. Finally the Pile-up noise contribution increases due to the higher luminosity as $\sqrt{L}$, but decreases due to shorter shaping times as $\sqrt{t}$. The final design was made for a shaping time of 400ns, assuming a luminosity of $\mathcal{L} \sim 2 \times 10^{32}\mathrm{cm}^{-2}\mathrm{s}^{-1}$. This leads to an electronic noise increase of a factor 1.6, an Uranium noise decrease of 2.3 and a pile-up noise increase of 1.3. The resulting noise performance is therefore comparable with the one achieved for the Run I conditions with the former electronics.

5 Summary

DØ is upgrading its detector: while the LAr calorimeter remains untouched, more severe machine conditions and the new environment (solenoid) necessite adaption of its electronics. An improved ICD coverage and modification in the scintillator read out will allow to maintain its performance. The new CPS and FPS detector will improve the electron and photon identification and restore energy losses in the increased material due to the solenoid.

Acknowledgments

Thanks to Ursula Bassler for her great help in finalizing the manuscript.

References

1. DØ Collaboration, "The DØ Upgrade: The Detector and Its Physics" (1996).
2. M. Adams et al., "Design Report of the Central Preshower Detector for the DØ Upgrade", DØ-note 3014 (1996).
3. A. Gordeev et al., "Technical Design Report of the Forward Preshower Detector for the DØ Upgrade" (1998).
4. A. Kotwal et al., "Calorimeter Electronics Upgrade for Run 2. Technical Design Report" (1998).